Flexible 3-D seismic survey design

Gabriel Alvarez[1]

ABSTRACT

Using all available subsurface information in the design of a 3-D seismic survey, we can better adjust the acquisition effort to the demands of illumination of the target horizon. I present a method that poses the choice of the acquisition parameters as an integer optimization problem. Rays are shot from grid points on the target reflector at uniform opening and azimuth angles and their emergence positions at the surface are recorded. The optimization (an exhaustive search in this example) minimizes the distance between the ray emergence coordinates and the source and receiver coordinates of candidate geometries subject to appropriate geophysical and logistics constraints. I illustrate the method with a 3-D subsurface model that I created featuring a target reflector whose depth changes significantly across the survey area. I show that for this model the standard approach would lead to a design requiring 200 shots/km^2 whereas the optimum design requires only 80 shots/km^2 without sacrificing the illumination of the target at any depth or the logistics of acquisition.

INTRODUCTION

For the design of a 3-D seismic survey to be effective, proper illumination of the target reflector and faults must be achieved. The mark of a successful design, however, is that it not only satisfies this condition, but provides for easy acquisition logistics with the lowest possible cost. The standard practice of 3-D seismic survey design assumes implicitly that the subsurface is composed of flat layers of constant velocity. Under this assumption, a set of source-receiver geometries have been devised and used extensively (Stone, 1994). These geometries usually correspond to parallel lines of receivers at fixed distances and to parallel lines of sources, also at fixed distances. The source lines are usually arranged parallel, perpendicular or slanted with respect to the receiver lines. Inasmuch as the assumption of flat parallel subsurface layers is valid, the design process can be standardized and can be seen as a somewhat routine application of known formulas to compute the distances between individual sources and receivers; separation between lines of sources and receivers; number of active channels per source and so on. Input information to the design process is limited to range of target depths and dips, maximum and minimum propagation velocities, and desired fold of coverage.

The key assumption of flat horizontal layers does not honor the complexity often present

[1]**email:** gabriel@sep.stanford.edu

in the geometry of subsurface layers in areas of great oil exploration or production interest. The survey designer usually ignores this discrepancy, however, partly because of mistrust of the available subsurface information and partly because of fear that exploiting that information may lead to ineffective logistics or may bias the results. Maintaining the assumption of flat layers is thus seen as a way to streamline the design process and to guarantee that the design is conservative with respect to our possibly inaccurate knowledge of the subsurface.

Survey designers often choose the source-receiver geometry from among the few standard geometries available (parallel, orthogonal, slanted, zig-zag) on the basis of uniformity of offset and azimuth in the subsurface bins (Galbraith, 1994). Wavefield sampling (Vermeer, 1998) may also be a consideration. In some cases, a 3-D subsurface model obtained from existing 2-D or 3-D data, well logs or geological plausibility is used to compute illumination maps of the reflectors of interest via forward modeling with various candidate geometries (Carcione et al., 1999; Cain et al., 1998). The geometry that provides the least distortion in illumination is chosen as the best design, after maybe tweaking it manually to fine tune its illumination response.

The methodology I propose for the optimization of the survey design poses the selection of the survey parameters as an optimization process that allows the parameters to vary spatially in response to changes in the subsurface. In a previous report (Alvarez, 2002b) I described the basic idea behind the method and illustrated it with a very simple 2-D synthetic model. In this paper I will illustrate the method in 3-D using a subsurface model I created to simulate a land survey. The emphasis will be on the description of the inversion to compute the parameters. I will show that a standard acquisition geometry will either sacrifice the offset coverage of the shallow part of the target horizon or require a large number of sources, which negatively impacts the cost of the survey. For the sake of simplicity, target depth was the only parameter I allowed to influence the spatial change of the geometry. Three geometries were computed according to the depth of the target reflector. Each geometry was locally optimized for uniformity of subsurface illumination. The optimum geometry, being more flexible, relaxes the acquisition effort without compromising the shallow part of the target reflector.

SUBSURFACE MODEL

To illustrate the method, I created a simplified subsurface model corresponding to a target horizon whose depth changes from about 0.3 km to about 2 km. The model simulates a land prospect, has high local dips and mild topography. Figures 1 and 2 show views of the model from the inline and the cross-line direction respectively. The model has significant dips in both directions. Similarly, Figures 3 and 4 show views of the target horizon from the inline and the cross-line direction. There are two possible reservoirs in this horizon, one at the top and one in the small structure to the right (Figure 4). The model is 10 km x 10 km with a maximum depth of about 3 km. The velocity field consists of blocks delimited by the reflectors. Within each block the velocity changes laterally as well as vertically in a gradient-based fashion as summarized on Table 1. Velocity at each point of each block is computed as $v(x,y,x) = v_0 + x\frac{\Delta v}{\Delta x} + y\frac{\Delta v}{\Delta y} + z\frac{\Delta v}{\Delta z}$.

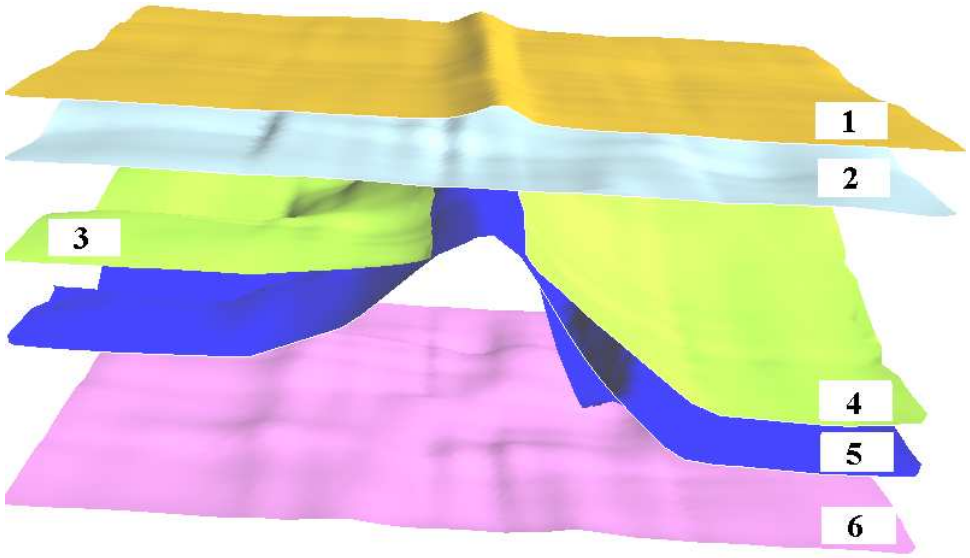

Figure 1: Subsurface model. View from the strike direction. The horizontal dimensions are 10 km x 10 km. The depth of the deepest reflector is 3 km. model1 [NR]

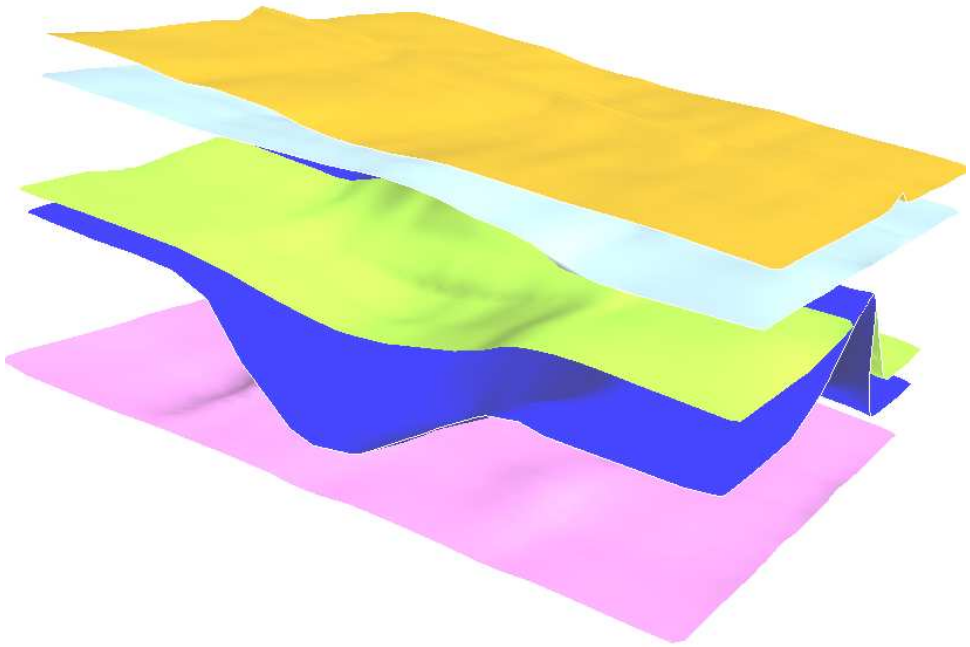

Figure 2: Subsurface model. View from the dip direction. The horizontal dimensions are 10 km x10 km. The depth of the deepest reflector is 3 km. model2 [NR]

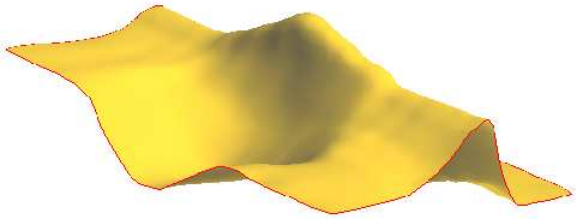

Figure 3: Target reflector. View from the dip direction. The reservoir corresponds to the top of the structure at a depth of about 0.3 km. target1 [NR]

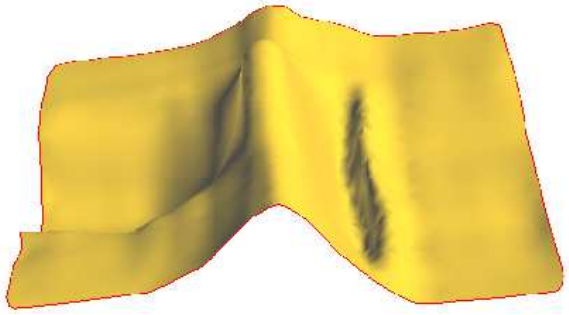

Figure 4: Target reflector. View from the strike direction. The reservoir corresponds to the top of the structure at a depth of about 0.3 km. target2 [NR]

STANDARD 3-D SURVEY DESIGN

Table 2 shows the input data for the standard design. The two most critical parameters, since they control the cost of the survey, are the maximum dip and the minimum target depth. The maximum dip controls the spatial sampling whereas the minimum target depth controls the separation between the receiver and shot lines as I will show below.

In Appendix A a give a fairly detailed description of the computation of the geometry parameters summarized on Table 2.

THE PROBLEM WITH THE STANDARD APPROACH

The survey parameters in Table 3 seem reasonable and well within the usual range, but there is a problem:

With an orthogonal geometry, there is a clear limit to the minimum offset that we can sample in all the bins as shown in Figure 5. The shortest offset in the central bin is approximately 700 m, which is too large compared to the depth of the shallowest part of the target reflector. With the basic assumption of flat layers and constant velocity, this means that the central bins will not have offsets short enough to image the shallow part of the target reflector. Since this is the main target, I can't afford to compromise its image. From Figure 5 it should be clear that in order to decrease the maximum minimum offset we need to decrease the source line interval, the receiver line interval or both. In this particular case, we can simply halve them so that the maximum minimum offset is now just over 300 m. Obviously, halving the dsl doubles the number of required shots which in turn may double the cost of the survey. Furthermore, if the number of receiver lines is kept constant (which may be necessary if not enough equipment is available) the aspect ratio will also double, making the survey highly azimuthal, which may

Table 1: Velocity information. Each block is delimited by two reflectors, numbered as indicated on Figure 1. Units are m/s.

Block	Reflectors	v_0	$\frac{\Delta v}{\Delta x}$	$\frac{\Delta v}{\Delta y}$	$\frac{\Delta v}{\Delta z}$
1	1 and 2	2000	0.01	0.05	0.5
2	2 and 3	3000	0.05	0.01	0.2
3	3 and 4	2400	0.01	0.01	0.5
4	4 and 5	3600	0.05	0.01	0.1
5	5 and 6	5000	0.0	0.0	0.0

Table 2: Input to the standard design.

V_{min}	θmax	$f$max	z_{min}	$z$max	$fold$
2000	60	60	300	3000	24

not be what we want. A possible solution is to use rectangular bins with the source interval equal to twice the receiver interval. This keeps both the number of shots and the aspect ratio constant, but may be an undesirable solution if significant dips are present in the strike direction (I am assuming that the source lines are in the strike direction).

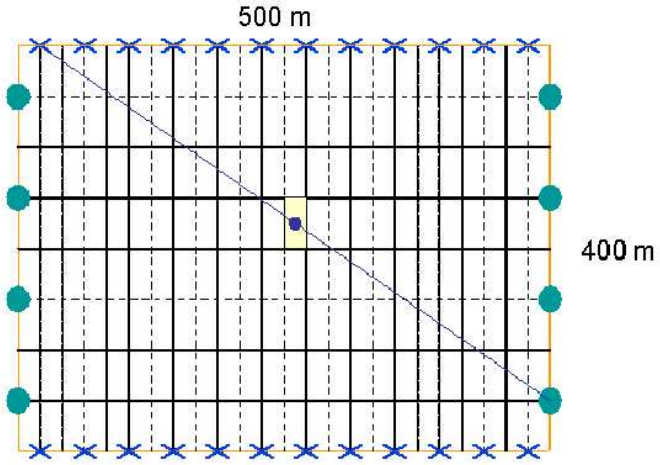

Figure 5: Recording box. Receivers are along the horizontal lines and sources along the vertical lines. The minimum possible offset for the bins in the middle of the box is of the order of 700 m, much too large to image the target reflector at 300 m depth. box1 [NR]

THE PROPOSED APPROACH

The message in the previous section was that the standard design approach incurs compromises between the requirements of image quality and the cost of the survey (and the amount of collected data). My proposed approach (Alvarez, 2002b) avoids those compromises by posing the design as an optimization problem in which the requirements of image quality and the

Table 3: Parameters of the standard design: dr is the receiver interval, ds is the source interval, drl is the receiver line interval, dsl is the source line interval, $nchl$ is the number of channels per line and nrl is the number of receiver lines in the recording patch. Units are meters.

dr	ds	drl	dsl	$nchl$	nrl
20	20	400	500	150	8

survey cost are balanced against each other within the constraint of sound acquisition logistics. Note that the compromises in the design stem from insufficient input data, or what amounts to the same thing, an inappropriate subsurface model. The implicit model of flat layers with constant velocities forces us to use the same acquisition parameters for the entire survey area. In the example described above, I "punished" the design because of the need to image the shallow part of the target horizon, although Figures 3 and 4 show that the target reflector is only shallow in about 10 or 20% of the survey area.

The upshot, of course, is that if we can accurately establish the correspondence between the subsurface area of the shallow reflector and the part of the surface area whose sources and receivers contribute to its image, then we could use the dense acquisition parameters in that part of the survey area and use the more standard parameters in the rest of the survey area. This is the key idea that allows us to get optimum image quality with the least acquisition effort. A similar approach can be used to locally increase the offsets for high-dipping reflectors, or to increase the azimuth coverage of a locally fractured reservoir.

I will illustrate in some detail each step of my approach with the model shown in Figures 1 and 2.

Building of the Model

I created the model from 5 cross-sections in the inline direction and 4 cross-sections in the cross-line direction using the Integra Software [2]. In this system the reflector surfaces are represented by B-splines which allows the accurate computation of the normal to the reflector at every point (Pereyra, 2000). In general, the structural and velocity model is constructed by integrating all available information from geology, well logs and previous 2D and 3D seismic data. The model does not need to be particularly detailed, although the main features are expected to be reasonably well represented. In the present case the model is not derived from any data and is purely conceptual.

[2]Developed by Weidlinger and Associates

Exploding Reflector Modeling

The subsurface model is used to trace rays up to the surface from points on the reflectors of interest at finely-sampled opening (polar) and azimuth angles. The number and location of the reflecting points on the reflectors of interest, as well as the number of rays shot from each such point, is a matter of design. The important point is that they represent our ideal subsurface illumination response. Departures from this ideal will be penalized in the optimization process. For this paper I used the Integra software to do the ray tracing. I used Gocad to compute a stratigraphic grid draped over the target reflector (Figure 4) and used the grid centers as the starting points for the rays. The grid is 25 x 25 m and 20 rays were shot from each point. The range of azimuths was from 0 to 135 degrees in intervals of 45 and the range of opening angles was from 0 to 60 degrees in intervals of 15 degrees. Figure 6 shows ray cones emanating from a few selected points on the target horizon's surface.

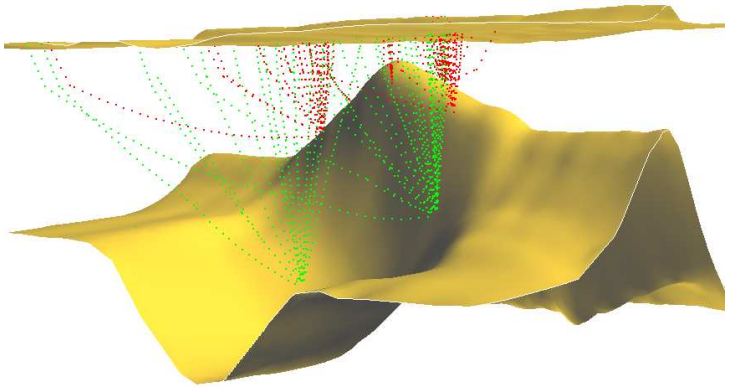

Figure 6: Exploding reflector rays. Rays from a few of the reflecting points on the target horizon. There are several thousand such reflecting points, so the resulting density of rays is very large. rays1 [NR]

Integra ray tracing program computes, for each ray, its travel time and the coordinates of the emerging point at the surface. The program also records the coordinates of the normal to the reflector at the starting point, as well as the opening and azimuth angle of the corresponding ray. In the present example I used this information to separate the rays originating at different depths in the target reflector.

Geometry Optimization

The most important part of my approach is using the information computed from the rays to optimize the layout of the sources and receivers. There are several ways in which this can be accomplished according to how much departure from the standard geometry we are prepared to accept.

1. Choose an orthogonal, parallel, or slanted geometry with parallel receiver lines as well as parallel source lines. In this case the optimization consists of choosing receiver and

shot sampling interval, receiver and source line separations, number of channels per active receiver lines and number of active receiver lines per shot. These parameters can be changed spatially to conform with the requirements of the image, but the basic geometry is unchanged. In other words, the optimum geometry is the composite of regular geometry patches each of which is optimum for a given part of the survey area.

2. Choose a dense receiver patch with similar receiver sampling in the inline and the cross-line direction and optimize the location of the shots which will not form continuous source lines. The source positions will be computed to optimize uniformity of the sub-surface illumination. Optimizing the source positions is particularly attractive in environments in which the layout of the receivers is easy but the drilling of shot holes is expensive. The use of vibrators may also be optimized, since the road paths can be used to constrain the source positions at the design stage.

3. Allow shots and receivers to be placed in geometries other than continuous source and receiver lines. The constraints of offset and azimuth distribution as well as inline and cross-line offset sampling migration requirements can then be explicitly posed as optimization constraints.

For the sake of this example, I used the first approach, which is the least ambitious.

Preprocessing

For each reflecting point and azimuth, rays corresponding to the same opening angle on opposite sides of the normal are linked together as dual rays. Rays whose emergence point (or that of its dual) fall outside the permit area for sources and receivers are discarded. Also discarded are rays for which the total traveltime is longer than the trace length. The remaining rays are assigned source or receiver positions according to the shortest distance between their emergence point and the closest source or receiver position for each geometry. Once a ray is classified as, say, source, its dual will be classified as receiver. Note that this classification is geometry-dependent. Figure 7 shows an example of the classification of a ray and its dual for two candidate geometries. The classification is done for all valid rays and the total distance that the emergence points have to be moved to conform with each geometry is recorded and saved. Minimizing this distance is equivalent to maximizing uniformity of illumination.

For each geometry, I compute and save all the relevant parameters such as fold of coverage, maximum and minimum maximum offsets, aspect ratio, number of receiver per patch, etc. This information is saved and will be used as geophysical constraints for the optimization as described below. I also compute all relevant statistics of each geometry, such as number of sources, number of receivers, and receiver- and source-line cuts. This information is used to apply logistic constraints to the optimization. The cost of the survey, in particular, may largely depend on those statistics.

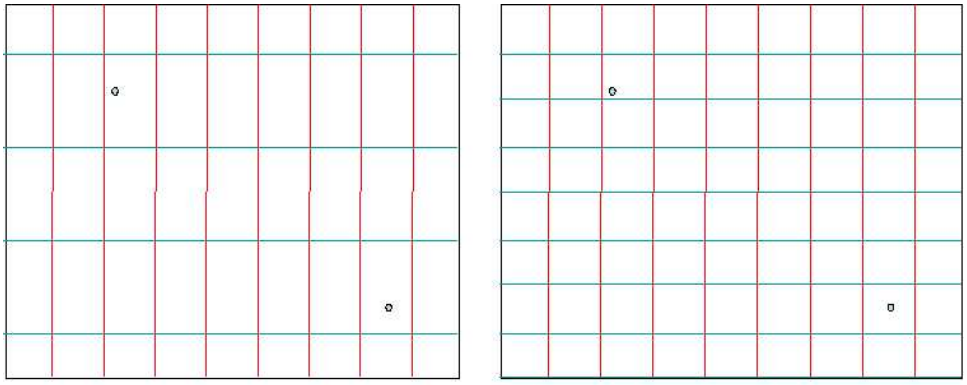

Figure 7: Classification of ray emergence points as sources or receivers. Vertical lines are source lines and horizontal lines are receiver lines. Two geometries are represented. The left panel illustrates a sparse geometry for which the ray in the top left would be classified as a source. The right panel shows the same ray which will now be classified as a receiver for this less sparse geometry. classify2 [NR]

Geophysical Constraints

In this case, by far the most important constraint was that the maximum minimum offset not be greater than the depth of the target reflector. The rays were split into three groups according to the depth of their reflecting point in the target reflector: from 300 to 400 m, from 400 to 700 m and deeper than 700 m. These ranges were chosen such that the densest acquisition is only used in the part of the surface that contributes the most to the image of the shallow part of the target horizon, and the coarser geometry be used in the part of the surface area that corresponds to the deeper parts of the target horizon with a transition zone in between. The different zones themselves were chosen according to the emergence coordinates of the normal rays. Figure 8 shows the three zones in map view superimposed on the topography. The dark shaded zone in the middle corresponds to the shallow part of the target horizon, the annular zone to the 400-700 meter depths and the darkest zone to the deeper parts of the target horizon. The important point is that this area is a small part of the total survey area. In fact, if we circumscribe a rectangle on this zone we find that its area is only about 3.5 km^2. Similarly, the area of zone 2 is about 7.5 km^2 which leaves zone 3 with an area of 89 km^2.

Another constraint was the aspect ratio of the recording patch. This is intended to maintain a range of short offsets where the reflector is shallow and longer offsets where the reflector is deeper. Also, this has the effect of avoiding abnormally high folds due to the contribution of long offsets that are not required where the reflector is shallow. Total fold was also considered a constraint to make sure that the minimum fold requirement is honored and to penalize geometries with much higher folds.

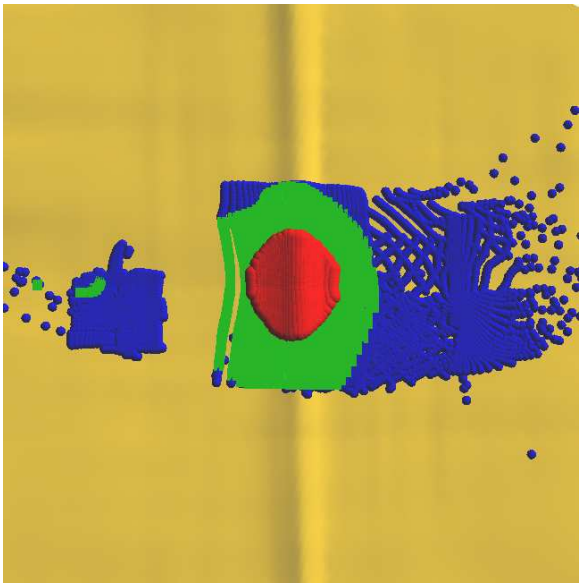

Figure 8: Survey area divided into three zones according to the depth of the target horizon. The dark shaded zone in the middle corresponds to the shallow part of the target horizon. The important point is that this area is a small part of the total survey area. zones1 [NR]

Logistic Constraints

Since in this case my trial geometries are completely regular, the only logistical constraint I applied was to ensure that the number of required channels satisfies the number of available channels in the candidate recording equipments for the acquisition of the survey. In particular, no penalty is given to a geometry that exactly matches the number of channels in any of the candidate recording equipments. Very high penalty is given to geometries that leave many channels unused and of course the highest penalty goes to any geometry that requires more channels than are available in any of the recording equipments. For example, if two recording equipments with 1000 and 2000 channels are available, a geometry that requires 900 channels is given a low penalty, one that requires 1100 channels is given a high penalty and one that requires more than 2000 channels is given the highest penalty.

The Optimization

Recall that in this case I chose to design the survey as a collection of three orthogonal surveys, the definition of each requiring only 5 parameters: source and receiver interval, source and receiver line interval and number of receiver lines per recording patch. Other considerations such as number of shots per salvo, number of stations to roll-along in the inline direction and number of receiver lines to roll-along in the x-line direction are also design parameters but I fixed them to be the number of shots between two adjacent receiver lines, the number of receivers between two adjacent source lines and one, respectively. The upshot is that the model space has only 5 parameters for each zone and an exhaustive search can be employed among all candidate geometries. In more irregular geometries, we may wish to invert for the parameters of each salvo and a micro-genetic algorithm (Alvarez, 2002a) will be a better choice.

The fitness function has two components: one to minimize the objectives and one to guarantee that the constraints are honored.

$$f_i = (1-\lambda)\sum_{j=1}^{m}\delta_j o_{ij} + \lambda\sum_{j=1}^{n}\epsilon_j c_{ij} \tag{1}$$

where i is the index that represents every trial geometry, λ is the factor balancing the two contributions to the fitness function, m is the number of objectives, o_{ij} is the figure of merit of the jth objective for ith geometry, δ_j is the relative weight of the jth objective, n is the number of constraints, ϵ_j is the relative weight of the jth constraint and c_{ij} is the figure of merit of the jth constraint for the ith geometry. In this case I chose $\lambda = 0.5$ which means that I am giving equal weight to the minimization of the objectives and to the satisfaction of the constraints.

The main objective, as mentioned before, is uniformity of target illumination, which requires minimization of the total distance that the emergence ray positions had to be moved to conform with each geometry. Also, since this is a land survey, the main factor in the cost of the survey is the number of shots. Therefore, I used the minimization of the number of shots as the second objective of the optimization. Finally, I used the total receiver- and source-line cut as additional, though less important, objective.

Notice that the constraints are not linear and that they may be partially fulfilled with partial penalties applied. The figures of merit assigned to the objectives and the constraints are normalized between 0 and 1, except when a constraint is completely violated, for example if the required number of channels is larger than the maximum number of available channels, as mentioned before. I made no attempt to differentiate cost between the available recording equipments although in practice this is likely to be an important issue.

The relative weights on each objective and on each constraint for the three zones are summarized on Table 4.

Table 4: Weights for the objectives and constraints applied in each zone: δ_1 is for illumination, δ_2 is for the number of shots, δ_3 is for receiver- and source-line cut, ϵ_1 is for maximum-minimum offset, ϵ_2 is for number of available channels, ϵ_3 is for aspect ratio and ϵ_4 is for fold of coverage.

Zone	δ_1	δ_2	δ_3	ϵ_1	ϵ_2	ϵ_3	ϵ_4
1	0.7	0.25	0.05	0.4	0.2	0.3	0.1
2	0.6	0.3	0.1	0.3	0.2	0.3	0.2
3	0.6	0.3	0.1	0.1	0.4	0.2	0.3

GEOMETRY WITH THE PROPOSED METHODOLOGY

As mentioned above, I subdivided the rays (and the survey area) into three groups. For each group I computed the optimum geometry using the corresponding subset of rays and the corresponding constraints as summarized in Table 5. The maximum minimum offset, the total fold

of coverage, the maximum offset and the aspect ratio were chosen differently for each zone. The source and receiver interval, however, were kept constant, meaning that the surface bins are the same, and were not included in the table. I did not apply any constraint to the offset or azimuth distribution in those bins, although I will implement that in the future.

Table 5: Constraints applied in each zone: c_1 is for maximum minimum offset, c_2 is for available channels, c_3 is for aspect ratio, and c_4 is for fold.

Zone	c_1	c_2	c_3	c_4
1	300-400	2000,3000,5000	1-3	24-36
2	500-600	2000,3000,5000	1-3	24-36
3	800-900	2000,3000,5000	1-2	24-32

I tried a total of 4608 geometries for each zone with parameter values as summarized on Table 6. Note that except for the receiver and group interval, the parameters are different in each zone. Also different are the constraints as shown in Table 5.

Table 6: Parameters for trial geometries in each zone. Units are in meters.

Zone	drl	dsl	nrl
1	300,320,340,360,380,400,420,440	300,320,340,360,380,400,420,440	6,8,10,12
2	380,400,420,440,460,500,540,580	380,400,420,440,460,500,540,580	4,6,8,10
3	540,560,580,600,640,680,720,760	540,560,580,600,640,680,720,760	4,6,8,10

Table 7: Parameters for the optimum geometry in each zone. Units are meters.

Zone	dr	ds	drl	dsl	nrl
1	20	20	380	320	12
2	20	20	380	440	10
3	20	20	760	720	10

The parameters of the resulting geometry for the three zones are summarized in Table 7. The parameters are significantly different, especially between zone 1, corresponding to the shallow part of the target horizon and zone 3 corresponding to the deep part of the same horizon. Notice that having these different parameters does not in itself compromise the logistics, since the distance between the receiver lines in zones 1 and 2 is half that in zone 3. In fact, for zone 3 the inversion gave me a handful of geometries that satisfied the objectives and the constraints equally and I chose the one that had this property. Logistically, all that would be required is to add an additional receiver line between two adjacent receiver lines in zones 1 and 2 assuming that we have enough equipment (and we do, since that was a constraint to the

inversion). The different separation of the source lines is even less of a problem since we can in principle drill the shot-holes along any line we want.

The bottom line

The bottom line in terms of cost of the survey, is that the standard dense geometry requires 200 shots/km^2 (50 shots/km and 4 receiver lines/km). For this model (100 km^2), this means 20000 shots which is extremely high. The optimum design uses the dense parameters 156 km^2 (50 shots/km and 3.125 receiver lines/km) only in zone 1, whose area is about 3.5 km^2; uses the intermediate design of 148 km^2 (50 shots/km and 2.95 receiver lines/km) only in zone 2 whose area is about 7.5 km^2*a*; and uses the sparse geometry of 70 km^2 (50 shots/km and 1.38 receiver lines/km) in the remaining 89 km^2. This gives a total of about 8000 shots, less than half those of the standard geometry. This saving in the number of shots is obtained without compromising the image of the target reflector at any depth and without significantly upsetting the logistics of the acquisition.

DISCUSSION

It is worth repeating that it is the simplicity of the flat layer model which makes the standard design approach so inflexible. This in turn forces compromises between the geophysical requirements of the survey and its cost. Moreover, since the geometry is fixed, subsurface variations would imply variations in the illumination as well. Exploiting all the available subsurface information has two main benefits: first, it allows target illumination to be the main goal of the design, and second it allows the geometry parameters to be locally optimum to satisfy the target local characteristics, such as depth, dip, curvature or presence of fractures.

Although not illustrated here, the resulting geometry should be used to compute illumination maps of the subsurface targets to make sure that the resulting illumination is indeed appropriate. If it is not, the density of rays in the problem areas may be increased and the process repeated perhaps with more relaxed constraints. Also, comparison with illumination maps computed with standard geometries should allow a better appreciation of the quality of the final design.

Different source-receiver geometries can be tested against each other by the optimization process, and, if desired, the optimum geometry can incorporate elements of each. Notice also that sources do not need to be along continuous lines (in land acquisition at least) and this fact can be exploited to improve the fit of the geometry to the emergence position of the rays, that is, to the illumination. The receivers are forced to be stringed together, but even so, we can use additional strings and stagger them to allow some flexibility without upsetting the logistics of the acquisition.

Another advantage of the methodology proposed here is the information we can gather about the relative contribution of each source (or group of sources), to the target illumination. This is important when we try to overcome obstacles that prevent us from placing sources or

receiver in their design positions. A river, for example, may force the displacement of sources or receivers several hundred meters. If the path of the river is known, we can use it as a constraint in the placement of sources and receivers in the optimization stage to compute the best geometry compatible with it. Even if we can't anticipate the presence of the obstacle at design time, we can still benefit from our knowledge of how much contribution the affected sources or receivers have on the target illumination. This information is of great help in choosing alternative positions to make up for those sources or receivers.

Finally, I would like to emphasize that the most important contribution of my methodology is *flexibility*. I have illustrated only one issue here, that of shallow targets, but you can easily think of other issues that would benefit from the more flexible approach. What constraints and what relative weights to assign to each one is clearly a problem-dependent decision and should reflect all the subsurface knowledge as well as the particulars of the survey.

CONCLUSION AND FUTURE WORK

I have illustrated my methodology for flexible survey design with an example in which a shallow reflector required a particularly dense acquisition geometry and have shown that it is possible to reduce considerably the number of sources by concentrating the acquisition effort where it is really required and relaxing it where is it safe to do so.

There are many issues that remain to be investigated, among them using the bin distribution of offsets and azimuths as constraints, considering multiple targets and non-standard geometries. The basic optimization method is already in place through the use of micro-genetic algorithms.

A critical issue to investigate is the influence of errors in the initial subsurface model in the computed geometry. Ultimately, I would like to quantify independently the influence of errors in reflector depths, reflector dips and velocities.

ACKNOWLEDGMENTS

I would like to express my deepest appreciation to Dr. Victor Pereyra for letting me use the Integra software for all the ray tracing in this paper. I would also like to thank Laura Carcione and Dr. Pereyra for teaching me the basics of the system and for providing me with advise and encouragement.

APPENDIX A

STANDARD GEOMETRY

Recording Geometry

To simplify the analysis I will assume an orthogonal split-spread geometry with the shot in the middle of the patch as is usual in land acquisition. I will not attempt to compare offset and azimuth distribution with other competing geometries such as parallel, slanted, or zig-zag but instead will assume that orthogonal geometry was already selected and that I just need to compute its parameters.

Bin size

The inline bin size is chosen from the sampling requirement to avoid aliasing of the steepest dip of interest. This requirement is represented by the equation

$$\Delta x \leq \frac{V_{\text{min}}}{2\, f_{\text{max}} \theta_{\text{xmax}}} \tag{A-1}$$

where V_{min} is the minimum velocity of interest, f_{max} the maximum frequency expected in the data and θ_{xmax} the maximum inline dip. With the values in Table 2, I got $\Delta x = 19$ which I will round to a standard value of 20 m. With this, the inline bin size is 10 m. I could use a similar computation to find the minimum cross-line sampling, but I will simply assume that the bin is square since the model is complex enough to have significant dips in directions other than the inline direction (Figures 1 and 2).

The bin size is thus 10x10 m and the source and receiver intervals are therefore both equal to 20 m.

Maximum offset inline and cross-line

The maximum offset inline essentially controls the maximum image depth and so can be chosen simply as the maximum depth of interest which in this case is 3000 m. The maximum cross-line offset controls the azimuth distribution of the traces in the subsurface bins. We want the acquisition effort to be concentrated on those azimuths more relevant to the image, but since in this case the model shows high dips in both directions, a wide azimuth distribution is desirable and therefore I choose the maximum cross-line offset also equal to 3000 m, that is, aspect ratio of one.

Source line and receiver line interval

In this case the desired fold for a 10 m x 10 m bin is 24. This fold can be decomposed as, say, 6 inline and 4 cross-line. Since the fold cross-line is half the number of receiver lines in

the recording patch, this means the recording patch will have 8 receiver lines. The distance between the receiver lines drl can be computed as

$$drl = \frac{2 * h_{\text{xmax}}}{nrl - 1} \tag{A-2}$$

where h_{xmax} is the maximum offset cross-line, 3000 m in this case, and nrl is the number of receiver lines per patch, 8 in this case. This gives $drl = 400m$.

The source line interval (dsl) can be similarly computed from the expectation that the inline fold be 6.

$$Fold_x = \frac{nchl\Delta x}{2dsl} \tag{A-3}$$

Here $nchl$ is the number of channels per receiver line, 300 in this case (maximum inline offset of 3000 m and receiver interval 20 m), Δx is the receiver interval, 20 m, and $Fold_x$ is 6. This gives $dsl = 500m$. If we wanted to apply the theory of symmetric wavefield sampling we might set $dsl = 400m$. Here I will not use the symmetric wavefield sampling theory.

Salvo

The salvo is the number of shots that are fired without moving the receiver template, so in this case it will be 20 shots since $drl = 400$ and $\Delta s = 20$.

REFERENCES

Alvarez, G., 2002a, Can we make genetic algorithms work in high-dimensionality problems?: SEP–**112**, 195–212.

Alvarez, G., 2002b, Toward subsurface illumination-based seismic survey design: SEP–**111**, 309–327.

Cain, G., Cambois, G., Gehin, M., and Hall, R., 1998, Reducing risk in seismic acquisition and interpretation of complex targets using a GOCAD-based 3-D modeling tool: 68th Annual Internat. Mtg., Society of Exploration Geophysicists, Expanded Abstracts, 2072–2075.

Carcione, L., Pereyra, V., Munoz, A., Ordaz, F., Torres, R., Yanez, E., and Yibirin, R., 1999, Model-based simulation for survey planning and optimization: 69th Annual Internat. Mtg., Society of Exploration Geophysicists, Expanded Abstracts, 625–628.

Galbraith, M., 1994, Land 3-D survey design by computer: , Austr. Soc. Expl. Geophys., Expl. Geophys., 71–78.

Pereyra, V., 2000, Ray tracing methods for inverse problems: Inverse Problems, **16**, R1–R35.

Stone, D., 1994, Designing seismic surveys in two and three dimensions: Society of Exploration Geophysicists.

Vermeer, G., 1998, 3-D symmetric sampling: Geophysics, **63**, no. 05, 1629–1647.